Passivity and Noncollocation in the Control of Flexible Multibody Systems

Christopher J. Damaren
Associate Professor,
Institute for Aerospace Studies,
University of Toronto,
4925 Dufferin Street,
Toronto, Ontario, M3H 5T6 Canada
e-mail: cjd@sdr.utias.utoronto.ca

Collocation of actuation and sensing in flexible structures leads to the desirable input-output property of passivity which greatly simplifies the stabilization problem. However, many control problems of interest such as robotic manipulation are noncollocated in nature. This paper examines the possibility of combining collocated and noncollocated outputs so as to achieve passivity. An appropriate combination is shown to depend on the interplay between collocated and noncollocated mass properties. Tracking problems are also studied and a controller with adaptive feedforward elements is introduced. An experimental study using a simple flexible apparatus with one rigid degree of freedom and two vibration modes is used to validate the analysis. [S0022-0434(00)01701-9]

1 Introduction

Many motion control problems are characterized by low mass structures which exhibit significant structural flexibility. There are often simultaneous requirements for control of rigid body motions coupled with active vibration suppression. Both problems are exacerbated by model uncertainty which necessitates the additional requirement of robustness.

It has long been known that robust stabilization of both rigid and flexible structures can be readily achieved by collocating dual sets of (rate) sensors and (force) actuators. In this case, the input-output (I/O) mapping is passive; in the linear time-invariant setting this manifests itself in the form of a positive real transfer function. Passivity and the positive real property were originally studied as characteristics of the driving point impedances of passive (for example, RLC) circuits [1]. Stabilization of passive systems is readily achieved using strictly passive feedback as predicted by the passivity theorem [2]. This stability property is robust because the passivity of the I/O map is independent of the structural details, manner of spatial discretization, and number of modeled modes, but merely resides in the collocation assumption. One of the first to realize this was Gevarter [3] who used simple proportional derivative (PD) laws and eigenvalue perturbation arguments.

Since then, many researchers have examined the collocated problem, but little research has investigated the exploitation of passivity for noncollocated inputs and outputs. Exceptions to this have typically focused on developing either static [4] or dynamic [5] output maps which yield a positive real system. In these cases, the required output transformation will be model dependent, but robustness can still be achieved by proper design of dynamic feedback compensation.

The simplest compensator achieving stabilization for a passive plant is positive rate feedback, but this must be extended to proportional-integral (PI or PD relative to position measurements) in the presence of rigid motions which lack stiffness. Benhabib et al. [6] emphasized that compensation in the form of strictly positive real (SPR) controllers could also furnish robust stability for passive systems and perhaps improve performance. Since then, many authors have established systematic procedures for SPR design [7–10].

Robotics problems, from the standpoint of joint-based control, furnish a class of systems exhibiting natural collocation and, although nonlinear, passivity has played an important role in the development of controllers for setpoint regulation [11] and both nonadaptive and adaptive tracking [12]. Space robotics has brought the problem of controlling flexible manipulators to the fore. In the archetypical form of the problem, one has a chain of flexible bodies with control inputs at the joints between bodies. However, the variables to be controlled are the position and orientation of the payload at the end of the manipulator. This represents a noncollocated problem requiring specialized approaches with serious limitations on achievable performance.

It was in the study of that problem that the present author examined the μ-output [13]. This is essentially a linear combination of collocated and noncollocated variables wherein $\mu=0$ yields the collocated case and $\mu=1$ gives the noncollocated one. The dependence of the passivity property on μ was studied in the asymptotic situation where the robot mass properties were negligible compared to those of the payload. Passivity was shown to be possible for $\mu<1$ and later work [14] showed that this bound prevails for planar two- or three-link flexible manipulators with large payloads and/or large stators present at the end of each link.

The present work serves to generalize the above by considering a finite noncollocated to collocated (generalized) mass ratio. This incorporates other important mass effects such as the lumped rotor inertias associated with highly geared actuators. A critical value, $\mu^\star$, is determined for which simple stabilization using the passivity theorem becomes possible for $\mu<\mu^\star$. In the case of multiple inputs and outputs, the analysis suggests the inclusion of a multiplier which defines the required spatial structure of the feedback controller. These enhancements greatly extend the applicability of the original ''large payload'' theory.

For simplicity, linearized dynamics are introduced in Sec. 2 which affords access to modal analysis and the frequency domain. Passivity is studied in Sec. 3 as a function of μ and the interplay between collocated and noncollocated mass distributions. In addition, a controller containing feedforward elements is presented in Sec. 4 which provides adaptive tracking for prescribed trajectories of a certain output. Experimental results from an apparatus with a single rigid rotational degree of freedom and two dominant vibration modes will be used in Sec. 5 to validate the analysis.

2 Motion Equations and Input-Output Model

The motions of a flexible structure are assumed to be governed by the standard second-order motion equation

$$\mathbf{M}\ddot{\mathbf{q}}+\mathbf{K}\mathbf{q}=\mathbf{B}\mathbf{f} \tag{1}$$

where **M, K**, and **B** are the mass, stiffness, and input matrices, respectively. The N generalized coordinates $\mathbf{q}$ and these matrices are assumed be partitioned as

Contributed by the Dynamic Systems and Control Division for publication in the JOURNAL OF DYNAMIC SYSTEMS, MEASUREMENT, AND CONTROL. Manuscript received by the Dynamic Systems and Control Division September 22, 1999. Associate Technical Editor: N. Olgac.

$$\mathbf{M}=\begin{bmatrix}\mathbf{M}_{\mathrm{rr}} & \mathbf{M}_{\mathrm{re}}\\ \mathbf{M}_{\mathrm{re}}^T & \mathbf{M}_{\mathrm{ee}}\end{bmatrix},\quad \mathbf{K}=\begin{bmatrix}\mathbf{O} & \mathbf{O}\\ \mathbf{O} & \mathbf{K}_{\mathrm{ee}}\end{bmatrix},\quad \mathbf{B}=\begin{bmatrix}\mathbf{1}\\ \mathbf{O}\end{bmatrix},\quad \mathbf{q}=\begin{bmatrix}\mathbf{q}_r\\ \mathbf{q}_e\end{bmatrix} \tag{2}$$

with $\mathbf{M}=\mathbf{M}^T>\mathbf{O}$ and $\mathbf{K}_{\mathrm{ee}}=\mathbf{K}_{\mathrm{ee}}^T>\mathbf{O}$. Hence, we identify $\mathbf{q}_r$ with the N_r rigid degrees of freedom, all of which are assumed to be actuated by N_r generalized forces $\mathbf{f}$. Rigid, as used here, denotes motions which are kinematically possible without storing any strain energy. The form of the input matrix $\mathbf{B}$ is consistent with the use of constrained (also called appendage) modes or more general constrained shape functions for the N_e elastic coordinates $\mathbf{q}_e$. That is, the elastic motions are kinematically subject to boundary conditions which are consistent with $\mathbf{q}_r(t)\equiv\mathbf{0}$. They correspond to motions which store strain energy in the system. The above description is sufficiently general to describe the linearized dynamics of an arbitrary elastic multibody system with complete actuation of the independent rigid degrees of freedom.

The output of interest is assumed to be of the form $\boldsymbol{\rho}_{\mathrm{nc}}(t)=[\mathbf{C}_r\mathbf{C}_e]\mathbf{q}(t)$ where it is assumed that $\mathbf{C}_r$ is square and invertible. In the case of a flexible manipulator, $\boldsymbol{\rho}_{\mathrm{nc}}$ would be the generalized tip position (relative to the linearization configuration) and $\mathbf{C}_r$ and $\mathbf{C}_e$ can be identified with the rigid and elastic Jacobian matrices. The subscript ''nc'' indicates ''noncollocated'' since, in general, the output of interest depends on $\mathbf{q}_e$ and hence is not collocated with the control inputs $\mathbf{f}$ (or $\mathbf{u}$). Although there may be other configuration variables that are not collocated, the term noncollocated will be reserved for this special output.

A more general output known as the μ-rate can be identified:

$$\mathbf{y}(t)=\dot{\boldsymbol{\rho}}_\mu\triangleq\mathbf{C}_r\dot{\mathbf{q}}_r+\mu\mathbf{C}_e\dot{\mathbf{q}}_e \tag{3}$$

where $\mu=1$ captures the true (noncollocated) rates, $\dot{\boldsymbol{\rho}}_{\mathrm{nc}}$, and $\mu=0$ constitutes an output $\dot{\boldsymbol{\rho}}_{\mathrm{co}}\triangleq\mathbf{C}_r\dot{\mathbf{q}}_r$ which is the natural dual of $\mathbf{u}(t)\triangleq\mathbf{C}_r^{-T}\mathbf{f}(t)$, an input more useful for our purposes. It is straightforward to show that $\dot{H}(\mathbf{q},\dot{\mathbf{q}})=\mathbf{u}^T\dot{\boldsymbol{\rho}}_{\mathrm{co}}=\mathbf{f}^T\dot{\mathbf{q}}_r$ where $H(\mathbf{q},\dot{\mathbf{q}})$ is the Hamiltonian corresponding to Eq. (1). Hence, $\mathbf{f}/\dot{\mathbf{q}}_r$ and $\mathbf{u}/\dot{\boldsymbol{\rho}}_{\mathrm{co}}$ form collocated I/O pairs. For control purposes, it is assumed that $\boldsymbol{\rho}_{\mathrm{nc}}$ and $\boldsymbol{\rho}_{\mathrm{co}}$ (via $\mathbf{q}_r$) can be measured so that $\boldsymbol{\rho}_\mu=\mu\boldsymbol{\rho}_{\mathrm{nc}}+(1-\mu)\boldsymbol{\rho}_{\mathrm{co}}$ can be formed.

The eigenproblem corresponding to Eq. (1) can be written as

$$-\omega_\alpha^2\mathbf{M}\mathbf{q}_\alpha+\mathbf{K}\mathbf{q}_\alpha=\mathbf{0},\quad \alpha=1,2,3,\ldots \tag{4}$$

where ω_α are the unconstrained vibration frequencies and the $\mathbf{q}_\alpha=\mathrm{col}\{\mathbf{q}_{r\alpha},\mathbf{q}_{e\alpha}\}$ provide the corresponding modes shapes. There are N_r zero-frequency rigid modes collectively of the form $\mathbf{Q}_r=[\mathbf{1}\quad\mathbf{O}]^T$. The modes enjoy standard orthonormality relations with respect to $\mathbf{M}$ and $\mathbf{K}$. Expanding the solution of Eq. (1) and the output in Eq. (3) in terms of eigenvectors, $\mathbf{q}(t)=\mathbf{Q}_r\boldsymbol{\eta}_r(t)+\Sigma_{\alpha=1}^{N_e}\mathbf{q}_\alpha\eta_\alpha(t)$, it is relatively straightforward to obtain the modal equations

$$\mathbf{M}_{\mathrm{rr}}\ddot{\boldsymbol{\eta}}_r=\mathbf{f}(t)=\mathbf{C}_r^T\mathbf{u}, \tag{5}$$

$$\ddot{\eta}_\alpha+\omega_\alpha^2\eta_\alpha=(\mathbf{C}_r\mathbf{q}_{r\alpha})^T\mathbf{u}(t),\quad \alpha=1,\ldots,N_e, \tag{6}$$

$$\mathbf{y}(t)=\mathbf{C}_r\dot{\boldsymbol{\eta}}_r+\sum_{\alpha=1}^{N_e}(\mathbf{C}_r\mathbf{q}_{r\alpha}+\mu\mathbf{C}_e\mathbf{q}_{e\alpha})\dot{\eta}_\alpha. \tag{7}$$

Using Laplace transforms, the dynamics of the system can be captured by the input-output description:

$$\mathbf{y}(s)=\mathbf{G}(s)\mathbf{u}(s), \tag{8}$$

$$\mathbf{G}(s)=\frac{1}{s}\mathbf{C}_r\mathbf{M}_{\mathrm{rr}}^{-1}\mathbf{C}_r^T+\sum_{\alpha=1}^{N_e}\frac{s}{s^2+\omega_\alpha^2}\mathbf{c}_\alpha\mathbf{b}_\alpha^T, \tag{9}$$

$$\mathbf{c}_\alpha=\mathbf{C}_r\mathbf{q}_{r\alpha}+\mu\mathbf{C}_e\mathbf{q}_{e\alpha},\mathbf{b}_\alpha=\mathbf{C}_r\mathbf{q}_{r\alpha}. \tag{10}$$

Recall that a general square system is strictly passive if $\int_0^{t_f}\mathbf{y}^T\mathbf{u}\,dt\geq\epsilon\int_0^{t_f}\mathbf{u}^T\mathbf{u}\,dt$ for some $\epsilon>0$, $\forall t_f\geq0$, and $\forall\mathbf{u}$ such that $\int_0^{t_f}\mathbf{u}^T\mathbf{u}\,dt<\infty$. The system is passive if $\epsilon=0$. For linear time-invariant systems, this is equivalent to positive realness of the corresponding transfer function $\mathbf{G}(s)$, i.e., $\mathbf{G}(s)$ is analytic and $\mathbf{G}(s)+\mathbf{G}^H(s)\geq\mathbf{O}$ for s in the open right-half plane.

The transfer matrix in Eq. (9) represents a linear combination of the positive real functions s^{-1} and $s/(s^2+\omega_\alpha^2)$. It is known [1] that such a function is positive real if and only if the coefficients, in this case $\mathbf{C}_r\mathbf{M}_{\mathrm{rr}}^{-1}\mathbf{C}_r^T$ and $\mathbf{c}_\alpha\mathbf{b}_\alpha^T$, are positive-semidefinite. Clearly the first of these is always so and the entire issue resides in identifying situations where $\mathbf{b}_\alpha\mathbf{c}_\alpha^T\geq\mathbf{O}$ for all modes. It occurs here for collocated feedback, i.e., $\mu=0$ so that $\mathbf{b}_\alpha=\mathbf{c}_\alpha=\mathbf{C}_r\mathbf{q}_{r\alpha}$. The next section serves to enlarge the range of μ leading to passivity which has the further advantage of introducing the noncollocated output into the feedback.

3 Perturbation Analysis, Multipliers, and Passivity

Let us explicitly indicate the portion of the mass distribution associated with the noncollocated motion, $\boldsymbol{\rho}_{\mathrm{nc}}$:

$$\mathbf{M}=\begin{bmatrix}\mathbf{C}_r^T\\ \mathbf{C}_e^T\end{bmatrix}\mathbf{M}_{\mathrm{nc}}[\mathbf{C}_r\quad\mathbf{C}_e]+\delta\mathbf{M} \tag{11}$$

where it is understood that $\delta\mathbf{M}$ can be partitioned analogously to $\mathbf{M}$ in Eq. (2). In other words, it is assumed that the kinetic energy can be written as

$$T=\tfrac{1}{2}\dot{\boldsymbol{\rho}}_{\mathrm{nc}}^T\mathbf{M}_{\mathrm{nc}}\dot{\boldsymbol{\rho}}_{\mathrm{nc}}+\tfrac{1}{2}\dot{\mathbf{q}}^T\delta\mathbf{M}\mathbf{q}.$$

The δ notation is used to indicate quantities that are small to first order; $\mathbf{M}_{\mathrm{nc}}>\mathbf{O}$ is $\mathcal{O}(1)$ and assumed to be the dominant contribution to the mass distribution. It is representative of a massive manipulated object such as a large payload at the end of a lightweight robotic manipulator. The eigenvectors $\mathbf{q}_\alpha$ are decomposed as

$$\mathbf{q}_\alpha=\overline{\mathbf{q}}_\alpha+\delta\mathbf{q}_\alpha \tag{12}$$

where $\overline{\mathbf{q}}_\alpha$ is $\mathcal{O}(1)$ and $\delta\mathbf{q}_\alpha$ denotes the first order perturbation due to $\delta\mathbf{M}$ which we seek to uncover. Both $\overline{\mathbf{q}}_\alpha$ and $\delta\mathbf{q}_\alpha$ can be partitioned analogously to $\mathbf{q}_\alpha$. The ensuing analysis is equivalent to taking $\delta\mathbf{M}$ ($\mathbf{M}$ less the $\mathbf{M}_{\mathrm{nc}}$ contribution) to be $\mathcal{O}(1)$ and taking $\mathbf{M}_{\mathrm{nc}}$ to be $O(\delta^{-1})$. In this light, $\overline{\mathbf{q}}_\alpha$ corresponds to the modes of the system with $\boldsymbol{\rho}_{\mathrm{nc}}=\mathbf{0}$ since as $\delta\to0$, the infinite contribution of $\mathbf{M}_{\mathrm{nc}}$ acts as a clamping boundary condition for $\boldsymbol{\rho}_{\mathrm{nc}}$.

The first row in eigenequation (4) implies that $\mathbf{M}_{\mathrm{rr}}\mathbf{q}_{r\alpha}+\mathbf{M}_{\mathrm{re}}\mathbf{q}_{e\alpha}=\mathbf{0}$ or, upon substitution of the relevant partitions in Eqs. (11) and (12),

$$(\mathbf{C}_r^T\mathbf{M}_{\mathrm{nc}}\mathbf{C}_r+\delta\mathbf{M}_{\mathrm{rr}})(\overline{\mathbf{q}}_{r\alpha}+\delta\mathbf{q}_{r\alpha})+(\mathbf{C}_r^T\mathbf{M}_{\mathrm{nc}}\mathbf{C}_e+\delta\mathbf{M}_{\mathrm{re}})(\overline{\mathbf{q}}_{e\alpha}+\delta\mathbf{q}_{e\alpha})=\mathbf{0}. \tag{13}$$

Expanding and collecting terms of like order gives to

$$\mathcal{O}(1):\qquad \mathbf{C}_r^T\mathbf{M}_{\mathrm{nc}}(\mathbf{C}_r\overline{\mathbf{q}}_{r\alpha}+\mathbf{C}_e\overline{\mathbf{q}}_{e\alpha})=\mathbf{0};$$

$$\mathcal{O}(\delta):\quad \mathbf{C}_r^T\mathbf{M}_{\mathrm{nc}}(\mathbf{C}_r\delta\mathbf{q}_{r\alpha}+\mathbf{C}_e\delta\mathbf{q}_{e\alpha})+\delta\mathbf{M}_{\mathrm{rr}}\overline{\mathbf{q}}_{r\alpha}+\delta\mathbf{M}_{\mathrm{re}}\overline{\mathbf{q}}_{e\alpha}=\mathbf{0}.$$

These imply that to

$$\mathcal{O}(1):\quad \mathbf{C}_r\overline{\mathbf{q}}_{r\alpha}=-\mathbf{C}_e\overline{\mathbf{q}}_{e\alpha}; \tag{14}$$

$$\mathcal{O}(\delta):\quad \mathbf{C}_e\delta\mathbf{q}_{e\alpha}=-[\mathbf{C}_r\delta\mathbf{q}_{r\alpha}+\mathbf{M}_{\mathrm{nc}}^{-1}\mathbf{C}_r^{-T}(\delta\mathbf{M}_{\mathrm{rr}}\overline{\mathbf{q}}_{r\alpha}+\delta\mathbf{M}_{\mathrm{re}}\overline{\mathbf{q}}_{e\alpha})]. \tag{15}$$

The first of these implies that the noncollocated output is ''clamped'' in each vibration mode to $\mathcal{O}(1)$ in keeping with the assumption that $\mathbf{M}_{\mathrm{nc}}$ forms the dominant contribution to the mass distribution. This follows from the definition of $\boldsymbol{\rho}_{\mathrm{nc}}$ which implies that $\mathbf{C}_r\overline{\mathbf{q}}_{r\alpha}+\mathbf{C}_e\overline{\mathbf{q}}_{e\alpha}$ is the relevant modal amplitude.

Using these expressions in Eq. (10), we can write

$$\mathbf{c}_\alpha \mathbf{b}_\alpha^T = \begin{cases} (1-\mu)(\mathbf{C}_r\overline{\mathbf{q}}_{r\alpha})(\mathbf{C}_r\overline{\mathbf{q}}_{r\alpha})^T, & \mathcal{O}(1); \\ (1-\mu)\mathbf{C}_r(\overline{\mathbf{q}}_{r\alpha}+\delta\mathbf{q}_{r\alpha})(\overline{\mathbf{q}}_{r\alpha}+\delta\mathbf{q}_{r\alpha})^T\mathbf{C}_r^T & \\ -\mu\mathbf{M}_{\mathrm{nc}}^{-1}\mathbf{C}_r^{-T}(\delta\mathbf{M}_{\mathrm{rr}}\overline{\mathbf{q}}_{r\alpha}+\delta\mathbf{M}_{\mathrm{re}}\overline{\mathbf{q}}_{e\alpha})(\overline{\mathbf{q}}_{r\alpha}+\delta\mathbf{q}_{r\alpha})^T\mathbf{C}_r^T, & \mathcal{O}(\delta), \end{cases} \tag{16}$$

where the second of these is correct to the indicated order. The $\mathcal{O}(1)$ result shows that $\mathbf{G}(s)$ in Eq. (9) is passive for $\mu<1$, but clearly ignores the correction stemming from $\delta\mathbf{M}$.

The inclusion of the $\delta\mathbf{M}$ effects in Eq. (16) can improve the estimate on the range of μ leading to passivity. However, the term containing $\delta\mathbf{M}_{\mathrm{re}}$ presents an obstacle to further analytical progress but can be neglected in some cases. Using Eq. (14), the bracketed expression in Eq. (16) containing $\delta\mathbf{M}_{\mathrm{re}}$ can be written as

$$\delta\mathbf{M}_{\mathrm{rr}}\overline{\mathbf{q}}_{r\alpha}+\delta\mathbf{M}_{\mathrm{re}}\overline{\mathbf{q}}_{e\alpha}=[\delta\mathbf{M}_{\mathrm{re}}-\delta\mathbf{M}_{rr}\mathbf{C}_r^{-1}\mathbf{C}_e]\overline{\mathbf{q}}_{e\alpha}$$

The term containing $\delta\mathbf{M}_{\mathrm{re}}$ can be neglected if $\|\delta\mathbf{M}_{\mathrm{rr}}\mathbf{C}_r^{-1}\mathbf{C}_e\| \gg \|\delta\mathbf{M}_{\mathrm{re}}\|$. This will happen when lumped rigid components associated with $\mathbf{q}_r$ alone dominate $\delta\mathbf{M}_{\mathrm{rr}}$. For example, rigid rotor inertias amplified by the use of large gear ratios contribute to $\delta\mathbf{M}_{\mathrm{rr}}$ but not $\delta\mathbf{M}_{\mathrm{re}}$.

The ensuing expression in (16) can be simplified by defining

$$\mathbf{M}_{\mathrm{co}} \triangleq \mathbf{C}_r^{-T}\delta\mathbf{M}_{\mathrm{rr}}\mathbf{C}_r^{-1}, \quad \mathbf{M}_t \triangleq \mathbf{M}_{\mathrm{nc}}+\mathbf{M}_{\mathrm{co}}, \tag{17}$$

$$\boldsymbol{\Upsilon}_\mu \triangleq [(1-\mu)\mathbf{1}-\mu\mathbf{M}_{\mathrm{nc}}^{-1}\mathbf{M}_{\mathrm{co}}], \tag{18}$$

$$\mathbf{c}_{r\alpha} \triangleq \mathbf{C}_r(\overline{\mathbf{q}}_{r\alpha}+\delta\mathbf{q}_{r\alpha}). \tag{19}$$

Notice that the collocated mass matrix $\mathbf{M}_{\mathrm{co}}$ represents the part of the mass distribution, less the $\mathbf{M}_{\mathrm{nc}}$ contribution, associated with $\boldsymbol{\rho}_{\mathrm{co}}$, assuming rigid bodies. Hence $\mathbf{c}_\alpha\mathbf{b}_\alpha^T=\boldsymbol{\Upsilon}_\mu\mathbf{c}_{r\alpha}\mathbf{c}_{r\alpha}^T$, $\mathbf{M}_{\mathrm{rr}}=\mathbf{C}_r^T(\mathbf{M}_{\mathrm{nc}}+\mathbf{M}_{\mathrm{co}})\mathbf{C}_r$, $\mathbf{C}_r\mathbf{M}_{\mathrm{rr}}^{-1}\mathbf{C}_r^T=\mathbf{M}_t^{-1}$, and using Eq. (9)

$$\mathbf{G}(s)=s^{-1}\mathbf{M}_t^{-1}+\boldsymbol{\Upsilon}_\mu\sum_{\alpha=1}^{N_e}\mathbf{c}_{r\alpha}\mathbf{c}_{r\alpha}^T\frac{s}{s^2+\omega_\alpha^2}. \tag{20}$$

In general, $\mathbf{G}$ is not positive real but the first term is and $\boldsymbol{\Upsilon}_\mu$ premultiplies a summation which also is.

The Single-Input Single-Output (SISO) Case (N_r=1). In this case note that

$$\Upsilon_\mu=1-\frac{\mu}{\mu^\star}, \quad \mu^\star \triangleq \frac{M_{\mathrm{nc}}}{M_{\mathrm{nc}}+M_{\mathrm{co}}}<1. \tag{21}$$

Therefore $G(s)$ is passive if and only if $\mu<\mu^\star$ When $\mu=\mu^\star$, the summation over the vibration modes vanishes (all vibration modes become unobservable) and the output $\dot{\boldsymbol{\rho}}_{\mu^\star}=\mathbf{C}_r\dot{\boldsymbol{\eta}}_r$ becomes proportional to the rigid body modal rate. It is instructive to consider a small negative rate feedback $\mathbf{u}(t)=-\epsilon\dot{\boldsymbol{\rho}}_\mu$. Using a simple eigenvalue perturbation argument, it is readily shown that the closed-loop eigenvalues of each vibration mode are given by $-\epsilon\Upsilon_\mu\mathbf{c}_{r\alpha}^T\mathbf{c}_{r\alpha}\pm j\omega_\alpha$. All modes are stabilized when $\mu<\mu^\star$ ($\Upsilon_\mu>0$) and all of them are destabilized when $\mu>\mu^\star$ ($\Upsilon_\mu<0$) assuming controllability and observability, i.e., $\mathbf{c}_{r\alpha}\neq 0$.

In Sec. 4, the tracking problem will be considered and one must decide which output is to be prescribed. On the basis of the above, $\boldsymbol{\rho}_{\mu^\star}$ is selected given the simple rigid nature of the I/O map. For $\mu<\mu^\star$, the I/O map is passive, hence minimum phase and causal inversion is possible. For $\mu>\mu^\star$, one expects nonminimum phase behavior and causal inversion would be impossible. In a certain sense, $\dot{\boldsymbol{\rho}}_{\mu^\star}$ is the closest output to $\dot{\boldsymbol{\rho}}_{\mathrm{nc}}$ whose I/O map can be inverted in a causal fashion. This will be further elucidated in Sec. 4.

The Multivariable Case (N_r>1). In the multivariable case, it is helpful to consider the (generalized) eigenproblem associated with the mass matrices:

$$\lambda_\alpha(\mathbf{M}_{\mathrm{nc}}+\mathbf{M}_{\mathrm{co}})\mathbf{e}_\alpha=\mathbf{M}_{\mathrm{nc}}\mathbf{e}_\alpha, \quad \alpha=1,\ldots,N_r. \tag{22}$$

Defining $\boldsymbol{\Lambda}_\mu \triangleq \mathrm{diag}\{\lambda_\alpha\}$ and $\mathbf{E}\triangleq\mathrm{row}\{\mathbf{e}_\alpha\}$, then with suitable normalization, $\mathbf{E}^T(\mathbf{M}_{\mathrm{nc}}+\mathbf{M}_{\mathrm{co}})\mathbf{E}=\mathbf{1}$ and $\mathbf{E}^T\mathbf{M}_{\mathrm{nc}}\mathbf{E}=\boldsymbol{\Lambda}_\mu$. Clearly $\lambda_\alpha>0$ and the eigenmatrix $\mathbf{E}$ will also diagonalize $\mathbf{M}_{\mathrm{co}}$. Using these relations, $\mathbf{M}_{\mathrm{nc}}^{-1}\mathbf{M}_{\mathrm{co}}=\mathbf{E}(\boldsymbol{\Lambda}_\mu^{-1}-\mathbf{1})\mathbf{E}^{-1}$ and from Eq. (18)

$$\boldsymbol{\Upsilon}_\mu=\mathbf{E}\boldsymbol{\Delta}_\mu\mathbf{E}^{-1}, \quad \boldsymbol{\Delta}_\mu \triangleq \mathbf{1}-\mu\boldsymbol{\Lambda}_\mu^{-1}=\mathrm{diag}\left\{1-\frac{\mu}{\lambda_\alpha}\right\}. \tag{23}$$

If μ is chosen to satisfy

$$\mu<\mu^\star \triangleq \min_\alpha \lambda_\alpha = \inf_{e\neq 0}\frac{\mathbf{e}^T\mathbf{M}_{\mathrm{nc}}\mathbf{e}}{\mathbf{e}^T\mathbf{M}_t\mathbf{e}}<\mathbf{1} \tag{24}$$

then $\boldsymbol{\Delta}_\mu$ is positive-definite. This definition of $\mu^\star$ generalizes that in Eq. (21).

Lemma 1. The transfer matrices $\hat{\mathbf{G}}=\mathbf{G}\boldsymbol{\Upsilon}_\mu^T$ and $\overline{\mathbf{G}}=\boldsymbol{\Upsilon}_\mu^{-1}\mathbf{G}$ are positive real if $\mu<\mu^\star$.

Proof. Given the expression in Eq. (20) both $\hat{\mathbf{G}}$ and $\overline{\mathbf{G}}$ are of the form $\mathbf{A}_0 s^{-1}+\Sigma_\alpha\mathbf{A}_\alpha s/(s^2+\omega_\alpha^2)$. It remains to show that $\mathbf{A}_0$ and the $\mathbf{A}_\alpha$ are positive-semidefinite in each case. For $\hat{\mathbf{G}}$, $\mathbf{A}_\alpha=\boldsymbol{\Upsilon}_\mu\mathbf{c}_{r\alpha}\mathbf{c}_{r\alpha}^T\boldsymbol{\Upsilon}_\mu^T\geqslant\mathbf{O}$ and for $\overline{\mathbf{G}}$, $\mathbf{A}_\alpha=\mathbf{c}_{r\alpha}\mathbf{c}_{r\alpha}^T\geqslant\mathbf{O}$. Now, note that $\mathbf{C}_r\mathbf{M}_{\mathrm{rr}}^{-1}\mathbf{C}_r^T=(\mathbf{M}_{\mathrm{nc}}+\mathbf{M}_{\mathrm{co}})^{-1}=\mathbf{E}\mathbf{E}^T$. Using this in conjunction with Eq. (23), $\mathbf{A}_0=\mathbf{C}_r\mathbf{M}_{\mathrm{rr}}^{-1}\mathbf{C}_r^T\boldsymbol{\Upsilon}_\mu^T=\mathbf{E}\boldsymbol{\Delta}_\mu\mathbf{E}^T$ for $\hat{\mathbf{G}}$, and for $\overline{\mathbf{G}}$, $\mathbf{A}_0=\boldsymbol{\Upsilon}_\mu^{-1}\mathbf{C}_r\mathbf{M}_{\mathrm{rr}}^{-1}\mathbf{C}_r^T=\mathbf{E}\boldsymbol{\Delta}_\mu^{-1}\mathbf{E}^T$. Both versions of $\mathbf{A}_0$ are positive-definite when $\mu<\mu^\star$ on account of $\boldsymbol{\Delta}_\mu>\mathbf{O}$. □

Application of the Passivity Theorem. Using the notion of multipliers [2], the feedback systems shown in Fig. 1 are equivalent from the point of view of stability. The passivity theorem states that if $\mathbf{G}$ is passive and $\mathbf{H}$ is strictly passive then $\mathbf{r}\in\mathbf{L}_2\Rightarrow\mathbf{y}\in\mathbf{L}_2$. Using Lemma 1 and the passivity theorem, the original system is stable if either $\hat{\mathbf{H}}=\boldsymbol{\Upsilon}_\mu^{-T}\mathbf{H}$ or $\overline{\mathbf{H}}=\mathbf{H}\boldsymbol{\Upsilon}_\mu$ is strictly passive. A possible design strategy would select $\mathbf{H}_{\mathrm{sp}}$, a strictly

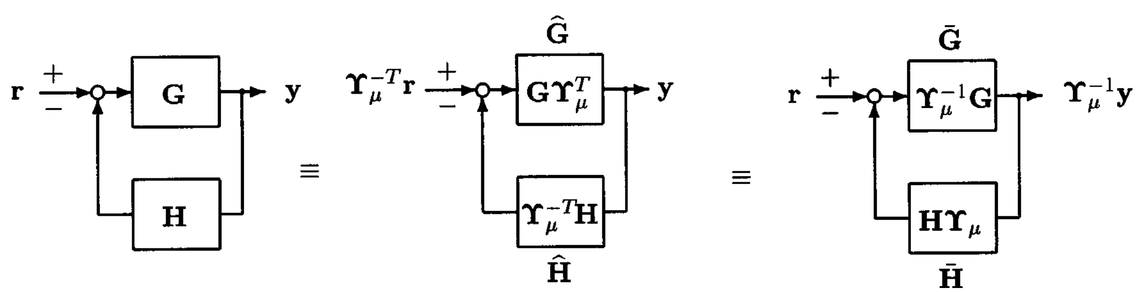

Fig. 1 Equivalent feedback loops

passive feedback, and then one would use either $\mathbf{H}=\mathbf{Y}_\mu^T\mathbf{H}_{\rm sp}$ or $\mathbf{H}=\mathbf{H}_{\rm sp}\mathbf{Y}_\mu^{-1}$. Either approach requires accurate knowledge of $\mathbf{M}_{\rm nc}$ and $\mathbf{M}_{\rm co}$ in forming $\mathbf{Y}_\mu$.

Alternatively, if $\mathbf{H}(s)=(K_d+K_p/s)\mathbf{M}_{\rm co}$ or $\mathbf{H}(s)=(K_d+K_p/s)\mathbf{M}_{\rm nc}$ where $K_p>0$, $K_d>0$, it is readily shown using the previous eigendecompositions that $\hat{\mathbf{H}}$ and $\overline{\mathbf{H}}$ are strictly passive since $\mathbf{Y}_\mu^{-T}\mathbf{M}_{\rm co}$ and $\mathbf{M}_{\rm nc}\mathbf{Y}_\mu$ are positive-definite matrices. The first of these is robust if $\mathbf{M}_{\rm nc}$ is poorly known and the second is robust if $\mathbf{M}_{\rm co}$ is poorly known. Both statements presuppose that μ is selected small enough. Other possibilities for $\mathbf{H}$ exist if the eigenstructure of $\mathbf{M}_{\rm nc}$ and $\mathbf{M}_{\rm co}$ is assumed known.

In summary, stabilization is possible using a PD law whose spatial structure mirrors that of $\mathbf{M}_{\rm nc}$ or $\mathbf{M}_{\rm co}$. This controller will be robust if $\mu<\mu^\star$ where $\mu^\star$ could be determined using an upper bound for $\mathbf{M}_{\rm co}$ or a lower bound for $\mathbf{M}_{\rm nc}$, respectively. The stability result is robust against variations in the stiffness properties and their manner of description but requires that $\|\delta\mathbf{M}_{rr}\mathbf{C}_r^{-1}\mathbf{C}_e\| \geqslant \|\delta\mathbf{M}_{re}\|$.

4 Feedforward Design and Adaptive Tracking

The development of a tracking controller is most readily accomplished in the time domain. A realization of the transfer matrix in Eq. (20) is given by

$$\mathbf{M}_t\ddot{\boldsymbol{\xi}}_r=\mathbf{u}(t), \tag{25}$$

$$\ddot{\boldsymbol{\eta}}_e+\boldsymbol{\Omega}_e^2\boldsymbol{\eta}_e=\overline{\mathbf{C}}_e^T\mathbf{u}, \tag{26}$$

$$\mathbf{y}(t)=\dot{\boldsymbol{\rho}}_\mu=\dot{\boldsymbol{\xi}}_r+\mathbf{Y}_\mu\overline{\mathbf{C}}_e\dot{\boldsymbol{\eta}}_e, \tag{27}$$

where $\boldsymbol{\eta}_e=\mathrm{col}\{\eta_\alpha\}$, $\boldsymbol{\Omega}_e=\mathrm{diag}\{\Omega_\alpha\}$, and $\overline{\mathbf{C}}_e=\mathrm{row}\{\mathbf{c}_{r\alpha}\}$. Ideally, we would like to find a control input $\mathbf{u}$ so that $\boldsymbol{\rho}_{\rm nc}$ tracks a desired trajectory $\boldsymbol{\rho}_d$ which is prescribed along with $\dot{\boldsymbol{\rho}}_d$ and $\ddot{\boldsymbol{\rho}}_d$.

To understand the difficulties associated with assigning $\boldsymbol{\rho}_d$ to the desired behavior of $\boldsymbol{\rho}_{\rm nc}$, let us adopt a quasistatic approximation for the elastic coordinates in Eq. (26), i.e., neglect $\ddot{\boldsymbol{\eta}}_e$. Such an approximation was shown to be highly effective in approximating the flexible motions produced by a complex simulation of the Space Shuttle Remote Manipulator System [13]. On this basis,

$$\boldsymbol{\eta}_e=\boldsymbol{\Omega}_e^{-2}\overline{\mathbf{C}}_e^T\mathbf{u}=\boldsymbol{\Omega}_e^{-2}\overline{\mathbf{C}}_e^T\mathbf{M}_t\ddot{\boldsymbol{\xi}}_r$$

where Eq. (25) has been used for $\mathbf{u}$. Substituting this into the integral of Eq. (27) gives

$$\boldsymbol{\rho}_\mu=\boldsymbol{\xi}_r+\mathbf{Y}_\mu\overline{\mathbf{C}}_e\boldsymbol{\Omega}_e^{-2}\overline{\mathbf{C}}_e^T\mathbf{M}_t\ddot{\boldsymbol{\xi}}_r$$

If $\boldsymbol{\rho}_d$ is assigned to the desired value of $\boldsymbol{\rho}_\mu$ ($\boldsymbol{\rho}_{\rm nc}$ when $\mu=1$), then the above ODE can be used to determine the desired trajectory for $\boldsymbol{\xi}_r$.

Assuming that $\boldsymbol{\rho}_d$ begins at $t=0$, a causal trajectory for $\boldsymbol{\xi}_r$ (i.e., one that also begins at $t=0$), depends on the stability of the ODE. To keep things simple, consider the SISO case and recall that $Y_\mu=1-(\mu/\mu^\star)$. Stability (causality of the I/O map from $\boldsymbol{\rho}_d$ to $\boldsymbol{\xi}_r$) requires that the coefficient of $\ddot{\boldsymbol{\xi}}_r$ above be positive which implies that $\mu<\mu^\star$. In general, a causal solution will not exist if $\mu=1>\mu^\star$, i.e., $\boldsymbol{\rho}_\mu=\rho_{\rm nc}$. However, for $\mu=\mu^\star$, $\boldsymbol{\rho}_\mu=\boldsymbol{\xi}_r$ since $Y_\mu=0$, so that the ρ_d can be identified with the desired behavior of the rigid (modal) coordinate $\boldsymbol{\xi}_r(t)$. Note that as $\mu^\star\to 1$, so that μ can be taken close to 1, $\boldsymbol{\rho}_\mu(t)\doteq\boldsymbol{\xi}_r(t)\doteq\boldsymbol{\rho}_{\rm nc}(t)$ and hence $\boldsymbol{\rho}_d$ is close to being the prescribed trajectory for $\boldsymbol{\rho}_{\rm nc}$.

Nonadaptive Case. Since $\boldsymbol{\rho}_d(t)$ is the desired trajectory for $\boldsymbol{\xi}_r(t)$, the nominal feedforward is selected to be $\mathbf{u}_d=\mathbf{M}_t\ddot{\boldsymbol{\rho}}_d$ according to Eq. (25). The desired behavior for the elastic coordinates, $\boldsymbol{\eta}_d$, is determined using Eq. (26):

$$\ddot{\boldsymbol{\eta}}_d+\boldsymbol{\Omega}_e^2\boldsymbol{\eta}_d=\overline{\mathbf{C}}_e^T\mathbf{u}_d. \tag{28}$$

This allows us to define the desired version of the μ-output,

$$\boldsymbol{\rho}_{\mu d}\triangleq\boldsymbol{\rho}_d+\mathbf{Y}_\mu\overline{\mathbf{C}}_e\boldsymbol{\eta}_d. \tag{29}$$

Setting $\tilde{\boldsymbol{\xi}}_r=\boldsymbol{\xi}_r-\boldsymbol{\rho}_d$, $\tilde{\boldsymbol{\eta}}_e=\boldsymbol{\eta}_e-\boldsymbol{\eta}_d$, $\tilde{\mathbf{u}}=\mathbf{u}-\mathbf{u}_d$, and $\tilde{\boldsymbol{\rho}}_\mu\triangleq\boldsymbol{\rho}_\mu-\boldsymbol{\rho}_{\mu d}$, it is clear that the dynamics relating $\tilde{\mathbf{u}}$ to $\dot{\tilde{\boldsymbol{\rho}}}_\mu$ are identical in form to those given by Eqs. (25)–(27) which relate $\mathbf{u}$ to $\mathbf{y}$. Thus, $\dot{\tilde{\boldsymbol{\rho}}}_\mu(s)=\mathbf{G}(s)\tilde{\mathbf{u}}$ and is governed by the passivity results of the previous section. Stabilization of the error dynamics is then possible by taking $\tilde{\mathbf{u}}=-\mathbf{Y}_\mu^T\mathbf{H}_{\rm sp}\dot{\tilde{\boldsymbol{\rho}}}_\mu$ so that

$$\mathbf{u}(t)=\mathbf{M}_t\ddot{\boldsymbol{\rho}}_d-\mathbf{Y}_\mu^T\mathbf{H}_{\rm sp}\dot{\tilde{\boldsymbol{\rho}}}_\mu. \tag{30}$$

Note that $\mathbf{H}_{sp}$ can simply be a PI law and $\boldsymbol{\rho}_\mu(t)$ can be formed from $\mu\dot{\boldsymbol{\rho}}_{\rm nc}+(1-\mu)\dot{\boldsymbol{\rho}}_{\rm co}$, thus avoiding measurements of $\boldsymbol{\eta}_e$.

Adaptive Case. In the case where $\mathbf{M}_t$ as needed in Eq. (30) is poorly known but we have a lower bound on $\mu^\star$, an adaptive tracking strategy can be established. The key resides in the notions of virtual trajectory and filtered error as originally introduced in a robotics context [12]. The desired feedforward is factored as $\mathbf{u}_d=\mathbf{M}_t\ddot{\boldsymbol{\rho}}_d=\mathbf{W}(\ddot{\boldsymbol{\rho}}_d)\mathbf{a}$ where the unknown, but assumed constant, parameters in $\mathbf{M}_t$ are contained in the column $\mathbf{a}$ and $\mathbf{W}$ is called the regressor matrix. Next, the virtual trajectory is defined by

$$\mathbf{v}_r=\dot{\boldsymbol{\rho}}_d-\boldsymbol{\Lambda}\tilde{\boldsymbol{\rho}}_\mu, \quad \boldsymbol{\Lambda}>\mathbf{O} \tag{31}$$

and the feedforward is modified to read

$$\mathbf{u}_d=\mathbf{W}(\dot{\mathbf{v}}_r)\mathbf{a}=\mathbf{M}_t(\ddot{\boldsymbol{\rho}}_d-\boldsymbol{\Lambda}\dot{\tilde{\boldsymbol{\rho}}}_\mu), \tag{32}$$

while $\boldsymbol{\eta}_d$ continues to be defined by Eq. (28). Subtracting Eq. (32) from Eq. (25) and Eq. (28) from Eq. (26), the error dynamics can be written as

$$\tilde{\boldsymbol{\rho}}_\mu=\tilde{\boldsymbol{\xi}}_r+\mathbf{Y}_\mu\overline{\mathbf{C}}_e\tilde{\boldsymbol{\eta}}_e, \quad \begin{cases}\mathbf{M}_t(\ddot{\tilde{\boldsymbol{\xi}}}_r+\boldsymbol{\Lambda}\dot{\tilde{\boldsymbol{\rho}}}_\mu)=\tilde{\mathbf{u}},\\ \ddot{\tilde{\boldsymbol{\eta}}}_e+\boldsymbol{\Omega}_e^2\tilde{\boldsymbol{\eta}}_e=\overline{\mathbf{C}}_e^T\tilde{\mathbf{u}}.\end{cases} \tag{33}$$

Consider the following Lyapunov-like function:

$$\mathcal{V}=\tfrac{1}{2}(\dot{\tilde{\boldsymbol{\xi}}}_r+\boldsymbol{\Lambda}\tilde{\boldsymbol{\rho}}_\mu)^T\mathbf{Y}_\mu^{-T}\mathbf{M}_t(\dot{\tilde{\boldsymbol{\xi}}}_r+\boldsymbol{\Lambda}\tilde{\boldsymbol{\rho}}_\mu)+\tfrac{1}{2}\dot{\tilde{\boldsymbol{\eta}}}_e^T\dot{\tilde{\boldsymbol{\eta}}}_e+\tfrac{1}{2}\tilde{\boldsymbol{\eta}}_e^T\boldsymbol{\Omega}_e^2\tilde{\boldsymbol{\eta}}_e\geqslant 0 \tag{34}$$

where $\mathbf{Y}_\mu^{-T}\mathbf{M}_t>\mathbf{O}$ since $\mathbf{M}_t^{-1}\mathbf{Y}_\mu^T>\mathbf{O}$ from the proof of Lemma 1. Using the error dynamics, its time derivative is $\dot{\mathcal{V}}=(\dot{\tilde{\boldsymbol{\rho}}}_\mu+\boldsymbol{\Lambda}\tilde{\boldsymbol{\rho}}_\mu)^T\mathbf{Y}_\mu^{-T}\tilde{\mathbf{u}}$. Integration of this relationship establishes passivity between $\mathbf{Y}_\mu^{-T}\tilde{\mathbf{u}}$ and $\mathbf{s}_\mu\triangleq\dot{\tilde{\boldsymbol{\rho}}}_\mu+\boldsymbol{\Lambda}\tilde{\boldsymbol{\rho}}_\mu$ which is termed the filtered error. If $\mathbf{Y}_\mu^{-T}\tilde{\mathbf{u}}$ is a strictly passive function of $-\mathbf{s}_\mu$ then $\mathbf{s}_\mu\in\mathbf{L}_2$. Using a well-known result, so are $\dot{\tilde{\boldsymbol{\rho}}}_\mu$ and $\tilde{\boldsymbol{\rho}}_\mu$. Hence, $\ddot{\boldsymbol{\rho}}_d$ can be replaced with $\dot{\mathbf{v}}_r$ and $\dot{\tilde{\boldsymbol{\rho}}}_\mu$ with $\mathbf{s}_\mu$ in Eq. (30) in the known parameter case:

$$\mathbf{u}(t)=\mathbf{M}_t\dot{\mathbf{v}}_r-\mathbf{Y}_\mu^T\mathbf{H}_{\rm sp}\mathbf{s}_\mu.$$

In the case where $\mathbf{a}$ is poorly known, an estimate $\hat{\mathbf{a}}(t)$ can be employed:

$$\mathbf{u}=\mathbf{W}(\dot{\mathbf{v}}_r)\hat{\mathbf{a}}+\overline{\mathbf{u}} \tag{35}$$

where $\overline{\mathbf{u}}$ is the feedback portion of $\mathbf{u}$. Subtracting Eq. (32) from Eq. (35) and defining $\tilde{\mathbf{a}}\triangleq\hat{\mathbf{a}}-\mathbf{a}$ gives $\mathbf{Y}_\mu^{-T}\tilde{\mathbf{u}}=\mathbf{Y}_\mu^{-T}[\mathbf{W}(\dot{\mathbf{v}}_r)\hat{\mathbf{a}}+\overline{\mathbf{u}}]$, which we would like to be a strictly passive function of $-\mathbf{s}_\mu$, i.e.,

$$-\int_0^{t_f}\mathbf{s}_\mu^T\mathbf{Y}_\mu^{-T}\tilde{\mathbf{u}}\,dt=-\int_0^{t_f}\tilde{\mathbf{a}}\mathbf{W}^T(\dot{\mathbf{v}}_r)^T\mathbf{Y}_\mu^{-1}\mathbf{s}_\mu\,dt-\int_0^{t_f}\mathbf{s}_\mu^T\mathbf{Y}_\mu^{-T}\overline{\mathbf{u}}\,dt$$

$$\geqslant\epsilon\int_0^{t_f}\mathbf{s}_\mu^T\mathbf{s}_\mu\,dt. \tag{36}$$

To this end, select

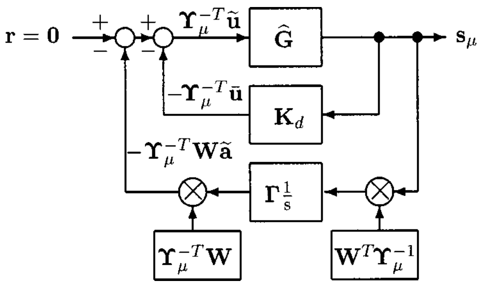

Fig. 2 Adaptive controller

$$\overline{\mathbf{u}} = -\boldsymbol{\Upsilon}_\mu^T \mathbf{K}_d \mathbf{s}_\mu \quad (\mathbf{K}_d > \mathbf{O}),$$

$$\dot{\tilde{\mathbf{a}}} = \dot{\hat{\mathbf{a}}} = -\boldsymbol{\Gamma}\mathbf{W}^T(\dot{\mathbf{v}}_r)\boldsymbol{\Upsilon}_\mu^{-1}\mathbf{s}_\mu \quad (\boldsymbol{\Gamma} > \mathbf{O}). \tag{37}$$

The first of these is strictly passive and the second represents a passive map ($\boldsymbol{\Gamma}s^{-1}$) from $\mathbf{W}^T\boldsymbol{\Upsilon}_\mu^{-1}\mathbf{s}_\mu$ to $\tilde{\mathbf{a}}$. The overall system is shown in Fig. 2 and represents the negative feedback interconnection of a passive system (the feedback interconnection of $\hat{\mathbf{G}}$ and the bottom adaptive loop, both of which are passive) and a strictly passive system $\mathbf{K}_d$. Hence, $\mathbf{s}_\mu \in \mathbf{L}_2$ and therefore $\tilde{\boldsymbol{\rho}}_\mu$, $\dot{\tilde{\boldsymbol{\rho}}}_\mu \in \mathbf{L}_2$ so that $\tilde{\boldsymbol{\rho}}_\mu(t) \to \mathbf{0}$ as $t \to \infty$. Further arguments can be used to show that $\dot{\tilde{\boldsymbol{\rho}}}_\mu$, $\tilde{\boldsymbol{\xi}}_r$, and $\tilde{\boldsymbol{\eta}}_e$ vanish as $t \to \infty$.

Implementation Issues. In the adaptive case, $\mathbf{M}_{\mathrm{nc}}$ is assumed unknown and therefore so is $\boldsymbol{\Upsilon}_\mu = \mathbf{1} - \mu(\mathbf{1} - \mathbf{M}_{\mathrm{nc}}^{-1}\mathbf{M}_{\mathrm{co}})$ which is required to form the feedback and adaptation laws in Eq. (37). However, if $\boldsymbol{\Upsilon}_\mu^T\mathbf{K}_d = K\mathbf{M}_{\mathrm{co}}$ $(K>0)$ which does not require $\mathbf{M}_{\mathrm{nc}}$ then $\mathbf{K}_d$ is positive-definite. The problem with the adaptation law can only be circumvented in certain cases. In the SISO situation, $\mathbf{W}^T = W$ and Υ_μ^{-1} commute so that Υ_μ^{-1} can be absorbed into the positive gain Γ. A similar possibility exists in the multiple input multiple output (MIMO) case if $\mathbf{M}_{\mathrm{nc}}$ and $\mathbf{M}_{\mathrm{co}}$ are diagonal so that $\mathbf{W}$ and $\boldsymbol{\Upsilon}_\mu$ can be taken to be diagonal. Otherwise, it is proposed to approximate $\boldsymbol{\Upsilon}_\mu$ by $(1-\mu)\mathbf{1}$ and absorb it into $\boldsymbol{\Gamma}$.

Another drawback is the calculation of $\boldsymbol{\eta}_d$ in Eq. (28) which requires $\mathbf{u}_d$ based on the true parameters. We propose to take $\boldsymbol{\rho}_{\mu d} \doteq \boldsymbol{\rho}_d$, an approximation which improves as $\mu \to \mu^\star$. The final form of the controller incorporating these modifications is

$$\mathbf{u}(t) = \mathbf{C}_r^{-T}\mathbf{f} = \hat{\mathbf{M}}_t[\ddot{\boldsymbol{\rho}}_d - \boldsymbol{\Lambda}(\dot{\boldsymbol{\rho}}_\mu - \dot{\boldsymbol{\rho}}_d)] - \mathbf{K}_d\mathbf{s}_\mu, \tag{38}$$

$$\dot{\hat{\mathbf{a}}} = -\hat{\boldsymbol{\Gamma}}\mathbf{W}^T(\dot{\mathbf{v}}_r)\mathbf{s}_\mu, \quad \hat{\boldsymbol{\Gamma}} = (1-\mu)\boldsymbol{\Gamma}, \tag{39}$$

where $\mathbf{s}_\mu = \dot{\tilde{\boldsymbol{\rho}}}_\mu + \boldsymbol{\Lambda}\tilde{\boldsymbol{\rho}}_\mu$ with $\tilde{\boldsymbol{\rho}}_\mu = \boldsymbol{\rho}_\mu - \boldsymbol{\rho}_d$.

5 Experimental Results

The control strategy developed in the previous section was implemented on the Torsional Control System apparatus developed by Educational Control Products. It consists of three concentric disks which are separated by two thin steel wires of length 305 and 310 mm (see Fig. 3). The wires are effectively modeled as massless lumped torsional stiffnesses k_1 and k_2. Each of the three disks can be removed or augmented with brass masses of variable position which allows one to systematically vary the axial moment of inertia of each disk (J_1, J_2, J_3).

The base disk is free to rotate and is driven by a brushless DC motor. Angular encoders (4000×4 counts per revolution) are used to sense the rotational motion of each disk $(\theta_1, \theta_2, \theta_3)$. Torque control of the motor is accomplished with a high gain PI current loop which has a bandwidth of 500 Hz. The apparatus is interfaced to a DSP which resides on the PC backplane and user written control algorithms can be developed on the PC and downloaded to the DSP.

If $q_r = \theta_1$, $q_{e1} = \theta_2 - \theta_1$, and $q_{e2} = \theta_3 - \theta_2$ are selected as generalized coordinates and $f(t)$ as the motor torque, the matrices defined in Eq. (2) are given by

$$\mathbf{M} = \begin{bmatrix} J_1+J_2+J_3 & J_2+J_3 & J_3 \\ J_2+J_3 & J_2+J_3 & J_3 \\ J_3 & J_3 & J_3 \end{bmatrix}, \quad \mathbf{K} = \begin{bmatrix} 0 & 0 & 0 \\ 0 & k_1 & 0 \\ 0 & 0 & k_2 \end{bmatrix},$$

$$\mathbf{B} = \begin{bmatrix} 1 \\ 0 \\ 0 \end{bmatrix}. \tag{40}$$

The noncollocated degree of freedom is taken to be $\rho_{\mathrm{nc}} = \theta_3 = \theta_1 + [1\ 1]\mathbf{q}_e$ so that $\mathbf{C}_r = 1$, $\mathbf{C}_e = [1\ 1]$. The collocated degree of freedom is $\rho_{\mathrm{co}} = \theta_1$ and $\rho_\mu = \mu\theta_3 + (1-\mu)\theta_1$.

Nominally, disks 1 and 2 were removed reducing J_1 and J_2 to their minimum values and the maximum number of masses (4) were placed on disk 3 in their most outboard position. The corresponding parameter values are given in Table 1. The calculated

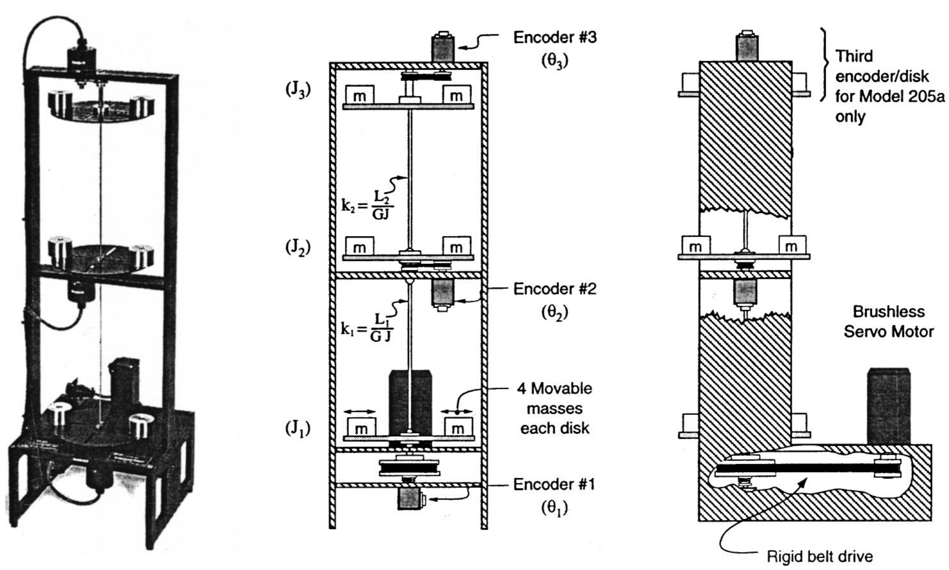

Fig. 3 Torsional control system apparatus (reprinted courtesy of Educational Control Products)

Table 1 Torsional apparatus parameter values

$k_1 = 2.8$ N·m/rad, $k_2 = 2.7$ N·m/rad
$J_1 = 0.508$ g·m^2, $J_2 = 0.008$ g·m^2, $J_3 = 18.725$ g·m^2

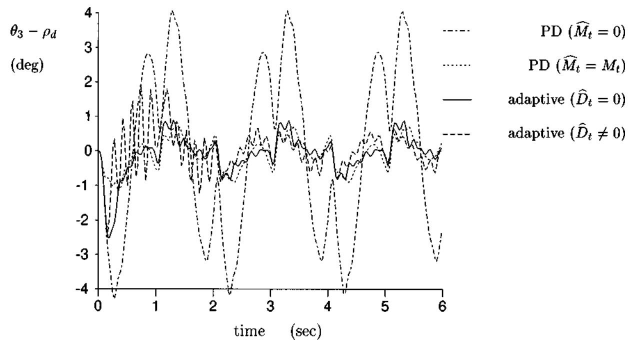

Fig. 4 Tracking errors ($\mu^\star = 0.973$, $\mu = 0.96$)

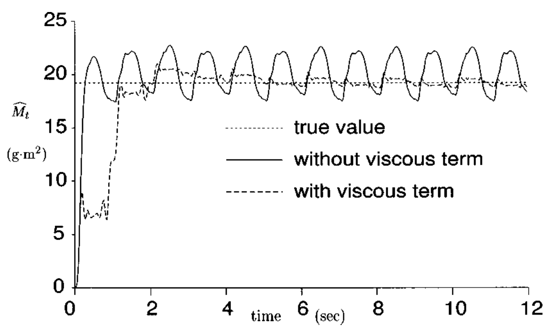

Fig. 5 Parameter estimates ($\mu^\star = 0.973$, $\mu = 0.96$)

natural frequencies for this configuration were $\omega_1 = 8.3$ Hz and $\omega_2 = 113$ Hz, both of which were validated experimentally to within 1%. For this structure $M_{\text{nc}} = J_3$ and $M_{\text{co}} = J_1 + J_2$ so that $\mu^\star = M_{\text{nc}}/(M_{\text{nc}} + M_{\text{co}}) = 0.973$ for the parameter values in Table 1.

All controllers were implemented with a sampling period of $T_s = 0.003536$ s and the derivatives $\dot{\theta}_1$ and $\dot{\theta}_3$ required to form $\dot{\rho}_\mu$ were obtained by simple differencing of the encoder measurements. Initially a PD law of the form $f(t) = -K_d s_\mu$, $s_\mu = \dot{\tilde{\rho}}_\mu + \Lambda \tilde{\rho}_\mu$, $\tilde{\rho}_\mu = \rho_\mu - \rho_d$ was employed with $K_d = 0.605$ N·m·s/rad/s, $\Lambda = 11.3$ s^{-1}, and $\rho_d = 0$. This places the eigenvalues of the rigid mode at $-15.7 \pm j10.4$ rad/s when $\mu = \mu^\star$. The stability boundary was found to occur experimentally at $\mu_{\text{cr}} = 0.973$ which is identical to the calculated value of $\mu^\star$.

For analysis of the tracking problem, the desired trajectory $\rho_d(t)$ was a quintic polynomial taking ρ_d from 0 to 180 deg in $T = 1$ s with $\dot{\rho}_d(0) = \dot{\rho}_d(T) = \ddot{\rho}_d(0) = \ddot{\rho}(T) = 0$. For 1 s$\leqslant t \leqslant$2 s, a similar maneuver takes ρ_d from 180 deg back to 0 and for $t \geqslant 2$ s, the entire maneuver repeats itself with a period of 2 s. The use of the simple PD law for tracking is shown in Fig. 4 ($\mu = 0.96$) and the tracking error is on the order of ± 4 deg. If this is augmented with the feedforward given in Eq. (30), i.e., $f(t) = M_t \ddot{\rho}_d - K_d s_\mu$, $M_t = J_1 + J_2 + J_3$, the tracking performance is greatly improved as shown in Fig. 4.

Setting $W(\ddot{\rho}_d) = \ddot{\rho}_d$, $a = M_t$, the adaptive form

$$f(t) = W(\dot{v}_r)\hat{a} - K_d s_\mu, \quad \dot{\hat{a}} = \Gamma W(\dot{v}_r) s_\mu \tag{41}$$

Table 2 Measured values of μ_{cr} at stability-boundary

J_1 (g·m^2)	J_2 (g·m^2)	J_3 (g·m^2)	$\mu^\star$	μ_{cr}
0.508	0.008	18.725	0.973	0.973
2.408	0.008	18.725	0.886	0.889
6.233	0.008	18.725	0.750	0.772
9.083	0.008	18.725	0.673	0.688
14.283	0.008	18.725	0.567	0.584
19.233	1.908	18.725	0.470	0.563
2.408	0.008	1.900	0.440	0.462
19.233	0.008	9.438	0.329	0.370
7.083	0.008	1.900	0.211	0.277
17.483	0.008	1.900	0.098	0.135

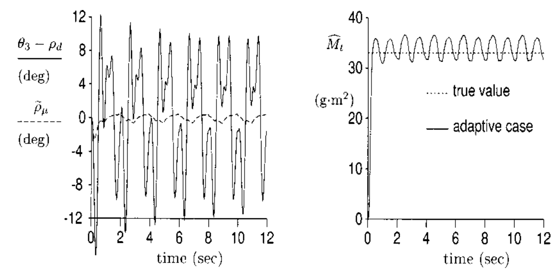

Fig. 6 Tracking errors and parameter estimates ($\mu^\star = 0.567$, $\mu = 0.55$)

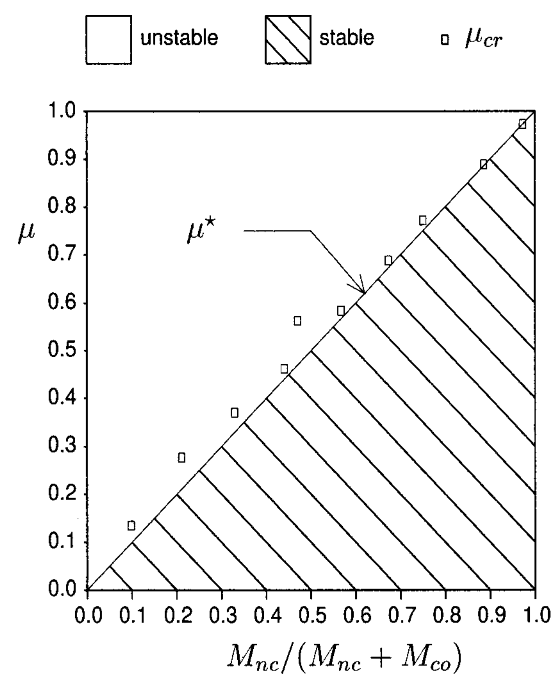

Fig. 7 Experimental and theoretical stability regions

was implemented with $\Gamma = 12.4$ g·m^2·s^2, which yields an average time constant for the adaptation of 0.63 s. The tracking performance for $\hat{a}(0) = 0$ is also given in Fig. 4 and is nearly as good as the fixed parameter case. This is excellent considering the speed of the maneuver and the flimsy nature of the structure separating the control input and the manipulated inertia. The behavior of the estimate $\hat{a}(t)$ is shown in Fig. 5. Notice that it oscillates about the true value on account of unmodeled effects such as drive and support joint friction. If this is modeled in the regressor by taking $\mathbf{W} = [\dot{v}_r \; v_r]$, $\hat{\mathbf{a}} = \text{col}\{\hat{M}_t, \hat{D}_t\}$ where $\hat{D}_t$ is interpreted as an effective viscous damping constant, the estimate $\hat{M}_t$ improves to that given in Fig. 5. The tracking error in Fig. 4 showed little change but further improvement is possible by attributing separate damping constants to $\dot{\theta}_1$ and $\dot{\theta}_3$.

Next, the controller in Eq. (41) was implemented for various values of J_1, J_2, and J_3 which were achieved by varying the location of the masses on J_3 and/or J_1. The critical value of $\mu^\star$ is tabulated in Table 2 along with the observed values of μ, μ_{cr}, which led to instability. In each case, stability was achieved for values of $\mu < \mu_{\mathrm{cr}}$. The agreement is quite good despite the fact that $\mu^\star$ was determined using first order perturbation theory which assumes that $M_{\mathrm{nc}} \gg M_{\mathrm{co}}$. The worst case occurs for $\mu^\star = 0.470$ which corresponds to including disk 2. This is not surprising since $\delta \boldsymbol{M}_{\mathrm{re}} = [J_2 \ 0]$ which was neglected in the analysis.

The tracking and adaptation performance are shown in Fig. 6 for the case where $\mu^\star = 0.567$ and a value of $\mu = 0.55$ was used. Notice that θ_3 tracks ρ_d to within 12 deg in the steady state, but one must bear in mind that ρ_d is the prescribed behavior of $\rho_{\mu^\star}$. The error $\tilde{\rho}_\mu$ is also shown in Fig. 6 and is considerably smaller.

The information conveyed by Table 2 in conjunction with Eq. (21) is summarized by the stability diagram in Fig. 7. Here, ''stable'' and ''unstable'' refer to the use of a strictly passive feedback and the values of μ_{cr} refer more specifically to the adaptive PD law used here. The most important feature of the diagram aside from the closeness of μ_{cr} and $\mu^\star$ is the conservative nature of the prediction from Eq. (21), i.e., $\mu^\star \leqslant \mu_{\mathrm{cr}}$ in all cases.

6 Concluding Remarks

A theory of control for flexible structures performing rigid body motions with noncollocated outputs and inputs has been presented. By judiciously combining collocated and noncollocated measurements, it has been shown that passivity can be achieved in the appropriate I/O map. Provided a lower bound on $\mu^\star$ is known, robust stabilization and tracking are possible using simple PD controllers.

An adaptive form of the tracking controller performed excellently for an experimental system with one rigid degree of freedom and all theoretical predictions were validated. The multivariable form of the control laws was established here and suggests the use of a PD controller whose feedback gains mirror the spatial structure of either the noncollocated or collocated mass matrix. Multibody problems with large rigid motions bring significant nonlinearities into play. Future work will address experimental implementation of the proposed controllers on flexible manipulators carrying large payloads.

Acknowledgment

The author gratefully acknowledges financial support provided by the University of Canterbury in the form of Research Grant 2201999.

References

[1] Newcomb, R. W., 1966, *Linear Multiport Synthesis*, McGraw-Hill, New York.
[2] Desoer, C. A., and Vidyasagar, M., 1975, *Feedback Systems: Input-Output Properties*, Academic Press, New York.
[3] Gevarter, W. B., 1970, ''Basic Relations for Control of Flexible Vehicles,'' AIAA J., **8**, pp. 666–672.
[4] Hughes, D., and Wen, J. T., 1996, ''Passivity Motivated Controller Design for Flexible Structures,'' AIAA J. Guid. Control Dynam., **19**, pp. 726–729.
[5] Lee, F. C., Flashner, H., and Safonov, M. G., 1995, ''Positivity-Based Control System Synthesis Using Alternating LMIs,'' *Proceedings of American Control Conference*, Seattle, WA, American Automatic Control Council, Evanston, IL, pp. 1469–1473.
[6] Benhabib, R. J., Iwens, R. P., and Jackson, R. L., 1981, ''Stability of Large Space Structure Control Systems Using Positivity Concepts,'' AIAA J. Guid. Control, **4**, pp. 487–494.
[7] McLaren, M. D., and Slater, G. L., 1987, ''Robust Multivariable Control of Large Space Structures Using Positivity,'' AIAA J. Guid. Control Dynam., **10**, pp. 393–400.
[8] Lozano-Leal, R. and Joshi, S. M., 1988, ''On the Design of Dissipative LQG-Type Controllers,'' *Proc. 27th IEEE Decision and Control Conference*, Dec., **2**, pp. 1645–1646.
[9] Haddad, W. M., Bernstein, D. S., and Wang, Y. W., 1994, ''Dissipative H_2/H_∞ Controller Synthesis,'' IEEE Trans. Autom. Control., **39**, pp. 827–831.
[10] Damaren, C. J., 1996, ''Gain Scheduled SPR Controllers for Nonlinear Flexible Systems,'' ASME J. Dyn. Syst., Meas., Control, **118**, pp. 698–703.
[11] Takegaki, M. and Arimoto, S., 1981, ''A New Feedback Method for Dynamic Control of Manipulators,'' ASME J. Dyn. Syst., Meas., Control, **103**, pp. 119–125.
[12] Ortega, R. and Spong, M. W., 1989, ''Adaptive Motion Control of Rigid Robots: A Tutorial,'' Automatica, **25**, pp. 877–888.
[13] Damaren, C. J., 1995, ''Passivity Analysis for Flexible Multilink Space Manipulators,'' AIAA J. Guid. Control Dynam., **18**, pp. 272–279.
[14] Damaren, C. J., 1998, ''Modal Properties and Control System Design for Two-Link Flexible Manipulators,'' Int. J. Robot. Res., **17**, pp. 667–678.